JOURNAL OF MAGNETIC RESONANCE **134,** 206–213 (1998)
ARTICLE NO. MN981502

Image-Based Reduction of Artifacts in Multishot Echo-Planar Imaging

Franciszek Hennel

MR Centre, FORENAP, 68250 Rouffach, France

Received December 22, 1997; revised April 6, 1998

The method to reduce the ghost artifact in echo-planar imaging (EPI) using a phase correction derived from the image data (M. H. Buonocore and L. Gao, *Magn. Reson. Med.* **38, 89 (1997)) is generalized to multishot (interleaved) EPI, where the artifact takes the form of multiple ghosts. The method is shown to be much more sensitive to noise when applied to standard interleaved data than is the case with single-shot EPI, because the calculation must be based on high-order ghosts of low intensity. A modified interleaving scheme is proposed for multishot EPI in which the initial trajectory direction alternates in consecutive shots and the number of shots is odd. With this scheme, only a single ghost shifted by one-half of the field of view appears just as in the single-shot EPI, and the image-based phase correction can be applied with the usual sensitivity to noise.**

Key Words: **echo planar imaging; interleaving; artifacts.**

INTRODUCTION

The echo-planar imaging (EPI) technique (*1, 2*) acquires the entire two-dimensional (2D) matrix of spatial frequency (*k*-space) data with a single train of gradient echoes generated by an oscillating readout gradient. The acquisition can be divided into a number of shots with interleaved *k*-space trajectories to reduce imaging distortion and minimize the loss of resolution caused by magnetic field inhomogeneity and transverse relaxation (*3, 4*). An inherent difficulty of EPI is a phase difference and a relative *k*-space shift of even and odd gradient echoes related to the fact that they are acquired with opposite polarities of the readout gradient. As a result, a ghost image appears shifted by one-half of the field of view (FOV) in the phase-encoding direction interfering with the original image and causing a loss of its amplitude (*5*). In multishot EPI the artifact takes the form of multiple ghosts distributed along the phase encoding direction (*3, 4*). To remove this artifact, a phase correction of either even or odd gradient echoes is required after the Fourier transformation (FT) in the readout direction and before the FT in the phase encoding direction. Phase correction parameters can be derived from a calibration scan performed without phase encoding, by comparison of phase spectra of even and odd echoes (*6*). Echo shifts are caused by a time lag of low-pass filters and by eddy currents induced with gradient switching. Therefore, phase correction parameters have to be measured anew, each time the orientation of the imaging plane, FOV, or sampling bandwidth is modified. To avoid the additional calibration scan, two (*7*) or more (*8*) dummy gradient echoes can be inserted into the sequence with phase encoding blips omitted. A drawback of this solution is a gap in the acquisition time which can become significant when a large number of interleaves (and a small number of echoes) is used.

However, as pointed out by Bruder *et al.* (*6*) and further developed by Buonocore and Gao (*9*), phase correction for single-shot EPI can be derived from the ghosted image data itself, provided the field of view in the phase encoding direction is greater than the object size. This method requires two separate 2D FTs of the *k*-space data, with odd and even rows masked by zeros, yielding two images $\rho_{\text{even}}(x, y)$ and $\rho_{\text{odd}}(x, y)$, respectively. Assuming for simplicity that the even echoes are correct and the odd ones are shifted, the two images can be expressed by

$$\rho_{\text{even}}(x, y) = \tfrac{1}{2}[\rho(x, y) + \rho(x, y - \text{FOV}/2)] \quad [1]$$

$$\rho_{\text{odd}}(x, y) = \tfrac{1}{2}[\rho(x, y) - \rho(x, y - \text{FOV}/2)]F(x), \quad [2]$$

where x and y are directions of the readout and phase encoding gradients, respectively, and $\rho(x, y)$ represents the original image. The factor $F(x)$ is a result of the inconsistency of even and odd echoes. In the case of odd echoes differing from the even ones by a phase offset of $2\pi a$ and a *k*-space shift of b, this factor takes the form

$$F(x) = e^{2\pi i(a+bx)}; \quad [3]$$

however, due to low-pass filtering, nonlinear phase terms can be introduced (*10*). Without any correction, the effective image is

$$\rho_{\text{even}}(x, y) + \rho_{\text{odd}}(x, y) = \tfrac{1}{2}[1 + F(x)]\rho(x, y) + \tfrac{1}{2}[1 - F(x)]\rho(x, y - \text{FOV}/2). \quad [4]$$

The two components represent the object and its ghost shifted

1090-7807/98 $25.00

by FOV/2, respectively. The correction requires an estimation of $F(x)$ by selecting a y_0 coordinate where the object is zero, but the ghost has a significant intensity (which is only possible when the y-size of the object is smaller than FOV) and taking a complex division of image rows

$$F_{\text{est}}(x) = -\rho_{\text{odd}}(x, y_0)/\rho_{\text{even}}(x, y_0). \quad [5]$$

A "deghosted" image can then be obtained by summing $\rho_{\text{even}}(x, y)\ F_{\text{est}}(x) + \rho_{\text{odd}}(x, y)$, or by multiplying even matrix rows by $F_{\text{est}}(x)$ between the FTs in the readout and phase encoding directions. Since the division is prone to errors due to noise, better results can be obtained by fitting a linear phase factor (Eq. [3]) to $F_{\text{est}}(x)/|F_{\text{est}}(x)|$ (*9, 11*).

In this note, we discuss the applicability of the image-based ghost reduction method to multishot EPI, where the phase difference of even and odd echoes leads to a multiple ghosting effect. It is shown that, although theoretically possible, the image-based reduction of multiple ghosting is much more sensitive to noise than is the case with the single ghost. A simple modification of the *k*-space interleaving scheme is proposed which converts the multiple-ghosting effect to a single ghost and allows the image-based correction method to be applied to multishot data with the same precision as in the single-shot EPI.

THEORY

Conventional Interleaving

In this chapter, we will derive expressions for two images reconstructed from only even and only odd gradient echoes of an interleaved EPI data set, and try to estimate the phase correction function in a way similar to that in single shot EPI. Again, it is assumed that the even echoes are correct and the phase error is attributed to the odd ones. The images reconstructed from even and odd echoes can be written as

$$\rho_{\text{even}}(x, y) = 2\text{DFT}[\, g_{\text{even}}(k_y)s(k_x, k_y)] \quad [6]$$

and

$$\rho_{\text{odd}}(x, y) = 2\text{DFT}[\, g_{\text{odd}}(k_y)s(k_x, k_y)]F(x), \quad [7]$$

where $s(k_x, k_y) = 2\text{DFT}^{-1}[\rho(x, y)]$ is the ideal, continuous *k*-space signal, and $g_{\text{even}}(k_y)$ and $g_{\text{odd}}(k_y)$ are the sampling distributions for even and odd echoes. We are discussing only the discrete sampling along the phase encoding direction; the sampling along the readout is treated as continuous. In the conventional interleaving scheme, *k*-space trajectories of consecutive shots are shifted in the phase encoding direction by one sampling unit $k_0 = 1/\text{FOV}$, otherwise being identical (Fig. 1a). This divides the *k*-space into blocks of n lines, n being the number of shots, which are sampled alternatively with left-oriented and right-oriented trajectory sections, corresponding to even and odd gradient echoes. Using Bracewell's symbols (*12*),

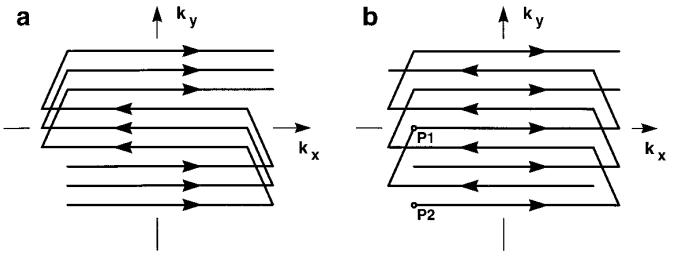

FIG. 1. *k*-space trajectories for a three-shot interleaved EPI sequence. (a) Standard interleaving; (b) interleaving with alternating initial direction.

$$\text{III}\left(\frac{k}{k_0}\right) = k_0 \sum_{m=-\infty}^{+\infty} \delta(k - mk_0) \quad [8]$$

and

$$\Pi(k) = \begin{cases} 1, & -\frac{1}{2} < k < \frac{1}{2} \\ 0, & \text{otherwise} \end{cases}, \quad [9]$$

the sampling distributions can be written as

$$g_{\text{even}}(k_y) = \frac{1}{k_0}\,\text{III}\left(\frac{k_y}{k_0}\right)\left[\,\Pi\left(\frac{k_y + d}{nk_0}\right) * \frac{1}{2nk_0}\,\text{III}\left(\frac{k_y}{2nk_0}\right)\right] \quad [10]$$

and

$$g_{\text{odd}}(k_y) = g_{\text{even}}(k_y + nk_0), \quad [11]$$

where * denotes a convolution in the k_y-dimension. The first III symbol in [10] represents *k*-space lines sampled at the k_0 interval. Symbol Π stands for a gate which selects one block of n lines. The gate is shifted by d to set its borders half way between two samples. Thus, $d = k_0/2$ for even n, and 0 for odd n. The convolution with the second III replicates this gate to all remaining even blocks. This sequence of operations is represented graphically in Fig. 2. The Fourier transforms in Eqs. [6] and [7] can be expressed by a y-convolution of $\rho(x, y)$ with the FTs of $g_{\text{even}}(k_y)$ and $g_{\text{odd}}(k_y)$, as calculated in the Appendix. We obtain

$$\rho_{\text{even}}(x, y) = \tfrac{1}{2}\,\rho(x, y) + \tfrac{1}{2}\sum_m A_m \rho\left[x, y - (2m + 1)\,\frac{\text{FOV}}{2n}\right] \quad [12]$$

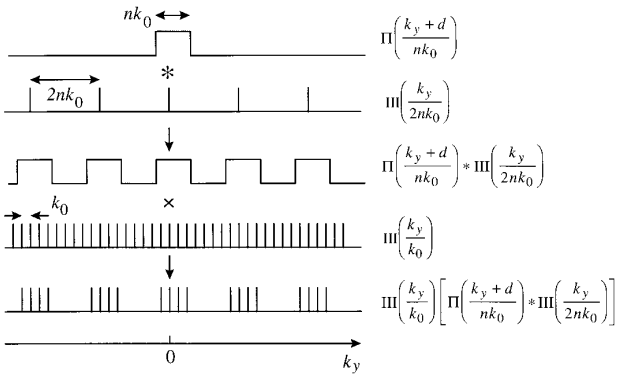

FIG. 2. Graphic representation of the sequence of operations in Eq. [10] describing the sampling distribution of even gradient echoes in interleaved EPI. Normalization constants are omitted for compactness.

$$\rho_{\text{odd}}(x, y) = \left\{ \tfrac{1}{2}\,\rho(x, y) - \tfrac{1}{2} \sum_m A_m \rho \times \left[x, y - (2m + 1)\,\frac{\text{FOV}}{2n} \right] \right\} F(x), \qquad [13]$$

where the summations include $m = -n/2 \ldots n/2 - 1$ (for n even), or $m = -(n - 1)/2, \ldots (n - 1)/2$ (for n odd). Both images consist of the original object and a train of ghosts shifted from the original by odd multiples of FOV/2n. The two images differ only by the sign of the train of ghosts and by the modulation resulting from the even–odd echo shift. Therefore, the modulation can be derived from these images in the same way as in single-shot EPI, i.e., using Eq. [5], with the y_0 line selected outside of the object and belonging to one or several ghosts. An example of a six-shot EPI image spoiled by the ghosting effect and corrected with the $F(x)$ correction derived from the artifact region is presented in Figs. 3a and 3b.

It should be noted, however, that the calculation of $F(x)$ is more difficult in the situation of multiple ghosts than it was with single-shot EPI. With single-shot data, the division in Eq. [5] involved ghost profiles whose amplitudes were identical with the original image. In multishot EPI, the amplitudes of the multiple ghosts are lower and decrease with the ghost order m as

$$|A_m| = |n \sin[\pi(2m + 1)/(2n)]|^{-1}. \qquad [14]$$

The strongest pair of ghosts ($m = -1, 0$) is about $2/\pi$ times weaker than the single artifact. However, these ghosts do not contribute significantly to the y_0 line, because they are shifted from the original by only FOV/2n. If the y_0 line is selected at the edge of the image and the object is centered in the field of view, as is typically the case, the ghost contributing most to y_0 is of order $m = n/2 - 1$ or $m = (n - 1)/2$, depending on the parity of n. The amplitude of this highest order ghost is about n times lower than the amplitude of the artifact in single-shot EPI. Therefore, when trying to estimate the phase correction in n-shot EPI, we have to perform a division of n-times lower profiles than would be the case with single-shot data. In practice, because of overlapping of several ghosts of different phases, the y_0 profile may be still weaker. One should thus expect the degree of error of the image-based phase correction of n-shot EPI to be the same as in a single-shot experiment with at least n times lower signal-to-noise ratio.

Another difficulty in the estimation of phase correction based on the even-echo and odd-echo images may arise from an instability of the NMR signal in consecutive shots, e.g., because of a lack of steady state of the longitudinal magnetization. If the signal amplitude is not constant in consecutive shots, the gate $\Pi(k)$ in Eq. [10] should be replaced by some other function which is also zero for $|k| > \frac{1}{2}$, but not flat inside. Following a similar analysis as in the Appendix, we will see that the even δ terms will not disappear in [A2], because the sinc will be replaced by some other function. Thus, the images calculated from even and odd echoes will contain both even and odd ghosts (precisely, ghosts shifted by even and odd multiples of FOV/2n):

$$\rho_{\text{even}}(x, y) = \sum_m B_m \rho\left[x, y - 2m\,\frac{\text{FOV}}{2n} \right] + \sum_m C_m \rho\left[x, y - (2m + 1)\,\frac{\text{FOV}}{2n} \right] \qquad [15]$$

$$\rho_{\text{odd}}(x, y) = \left\{ \sum_m B_m \rho\left[x, y - 2m\,\frac{\text{FOV}}{2n} \right] - \sum_m C_m \rho\left[x, y - (2m + 1)\,\frac{\text{FOV}}{2n} \right] \right\} F(x). \qquad [16]$$

It is important to note that the even ghosts have the same sign on both images. Therefore, to estimate the factor $F(x)$ using Eq. [5], one would have to find a y_0 coordinate at which only odd ghosts would be present and not the even ones, which is practically impossible. Figure 3c demonstrates the effect of superposition of odd and even ghosts caused by the even–odd echo shift and a lack of steady state of the longitudinal magnetization. The attempt to correct the echo shift using Eq. [5] fails in this case (Fig. 3c). We conclude that the odd ghosts caused by the even–odd echo shift in multishot EPI can be removed by the image-based phase correction under two conditions: sufficient signal-to-noise ratio and perfect stability.

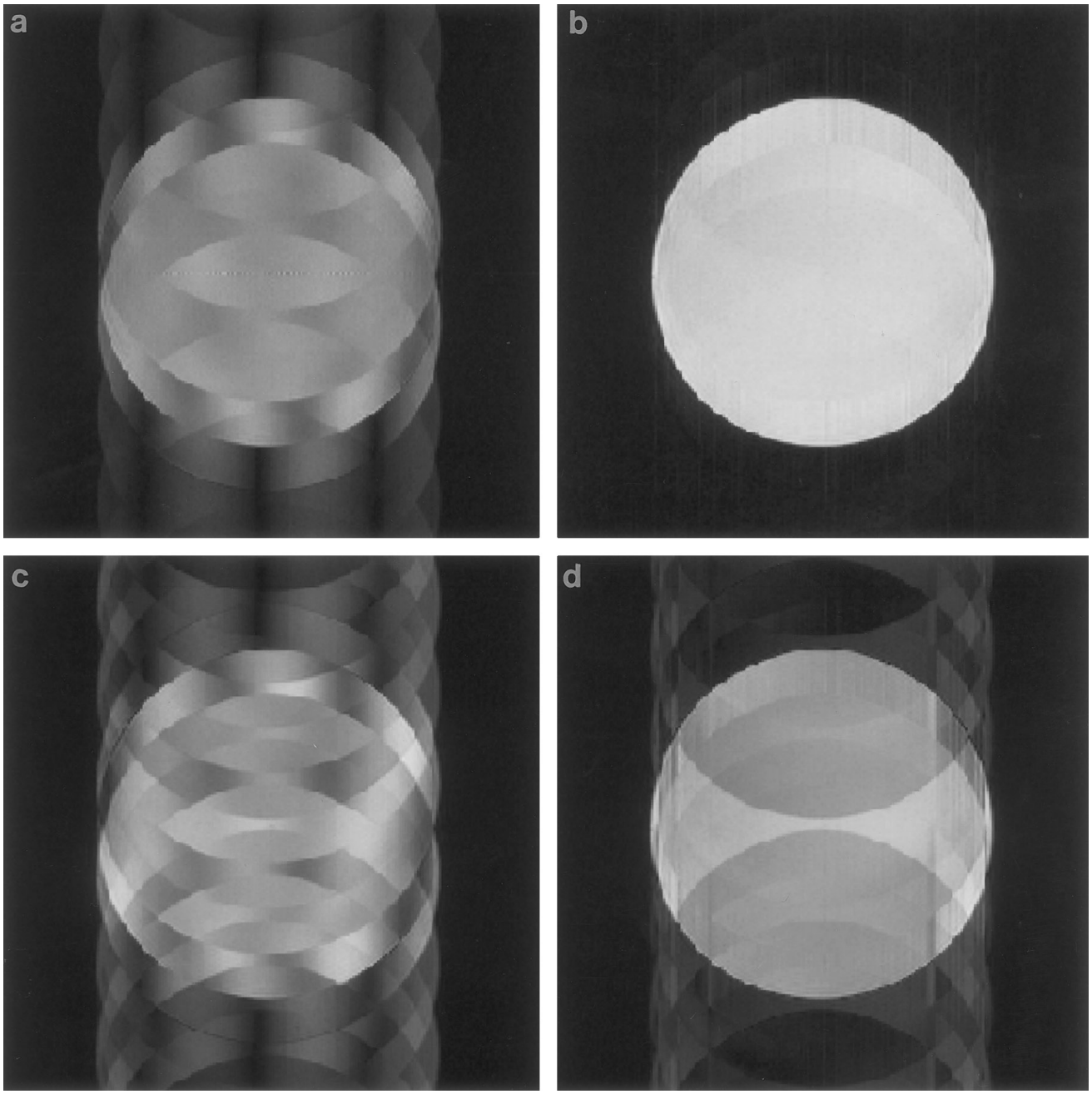

FIG. 3. Images of a spherical phantom obtained with a six-shot EPI sequence with standard interleaving: (a) image acquired in steady-state conditions with odd ghosts caused by a phase inconsistency of even and odd echoes; (b) the same data as (a), reconstructed with a phase correction derived from the artifact region using Eq. [5]; (c) second acquisition, in which the longitudinal magnetization was not in a steady state leading to additional even ghosts; (d) an attempt to correct (c) using a similar procedure fails because of the presence of even ghosts.

Contrarily to the description of ghosting effects in multishot EPI by Reeder *et al.* (*13*), the discrete Fourier transform was not applied explicitly in our analysis. Instead, transformation properties of sampling distributions in conjunction with the convolution theorem were used. It is possible, however, to derive Eqs. [12]–[14] from Eq. [A11] of Ref. *13*.

Alternating Interleaving

To restore the full sensitivity of the image-based phase correction method in multi-shot EPI, a modified *k*-space interleaving scheme is proposed. In addition to shifting of consecutive trajectories along k_y, the new scheme requires that the initial k_x-direction of the trajectories be alternated (Fig. 1b).

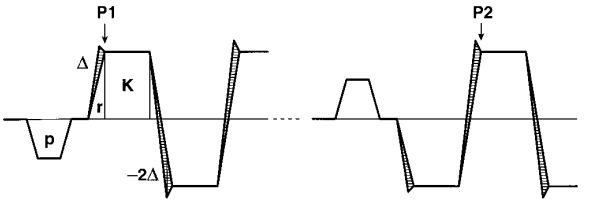

FIG. 4. Fragments of the readout gradient waveform in two consecutive shots with alternating trajectory direction. Dashed areas represent deviations from the ideal trapezoidal waveform. Points P1 and P2 correspond to markers on the trajectories in Fig. 1b.

Provided the number of shots is odd, this gives exactly the same situation as in single-shot EPI: even and odd *k*-space lines are scanned in opposite directions. Phase errors related to the scanning direction (i.e., to the polarity of the readout gradient) are again attributed to alternating lines. This can be expressed by setting $n = 1$ in Eqs. [12] and [13], which then become equivalent to the single-shot case (Eqs. [1] and [2]). Thus, with alternating directories, the phase errors lead to a single ghost that is shifted by FOV/2 and has the same amplitude as the original. The phase correction can now be estimated from Eq. [5] with the same sensitivity as in a single-shot experiment, disregarding the actual number of shots. Also, if even ghosts are present due to signal variations, they will have much less influence on the estimation of the phase correction, because their amplitude with respect to the odd ghost will be *n* times smaller. The only constraint of this solution is that the number of shots must be odd, meaning that the *y*-size of the data matrix cannot be a power of two, and that some zero-filling is necessary should the FFT algorithm be applied.

To implement this sampling scheme, the sign of the readout gradient waveform has to be alternated in consecutive shots, as shown in Fig. 4. It remains to be proven that echoes acquired with the same gradient polarity have an identical phase error and *k*-space shift in even and odd shots. Regarding the shift, the question can be put differently: do points P1 and P2 in Fig. 1b have the same k_x coordinate? The coordinate of P1 is given by the integral of the readout gradient from the beginning to the first plateau,

$$k_x(\mathrm{P1}) = p + r + \Delta, \qquad [17]$$

where p is the integral of the prefocusing lobe, r the nominal integral of one rising ramp, and Δ an unknown overshoot (or undershoot) caused by gradient amplifier or eddy currents. On the other hand, point P2 is at

$$k_x(\mathrm{P2}) = -p - r - \Delta - K + 2\Delta, \qquad [18]$$

where K is the integral of the readout plateau. A reasonable assumption has been taken here that the overshoot of the second ramp ($-\max \rightarrow +\max$) is twice the one of the first ramp ($0 \rightarrow +\max$). The two points have equal k_x coordinates when

$$p = -K/2 - r, \qquad [19]$$

which is when the echo is nominally centered at the readout plateau. Note that the integral of the prefocusing lobe can be set precisely because the overshoots of its rising and falling slopes compensate each other, so the condition of Eq. [19] can easily be fulfilled.

The same arguments apply to the zero-order phase shift of gradient echoes because this shift is caused by eddy-current-related pulses of the main magnetic field behaving just like the gradient ramp overshoots. Also, the nonlinear phase shifts caused by low-pass filters are directly related to the k_x-scanning direction. Thus, echoes scanned with the same polarity of the readout gradient are equivalent in alternate scans. In fact, this equivalence has already been used in an early two-shot variant of EPI (*14*).

IN VIVO RESULTS AND DISCUSSION

The image-based method for ghosting reduction was tested on *in vivo* data. The multishot EPI technique with standard and alternating interleaving schemes was installed on a whole-body 3-tesla MRI system (BRUKER Avance) equipped with a shielded gradient coil of 38 cm inner diameter. Axial images of the head of a healthy volunteer were acquired with a matrix of 240 × 234 points (readout × phase) in 9 shots of 26 gradient echoes using a spin-echo sequence with repetition time 3 s and echo time 80 ms. Fat signal was suppressed using a chemical-shift selective saturation pulse. Amplitude of the readout gradient was 9.6 mT/m, giving a field of view of 25.6 cm with 100 kHz sampling rate. Gradient switching time was 0.15 ms. Several dummy scans were performed to achieve a steady state of the longitudinal magnetization. Echo-time shifting was used to minimize phase discontinuities caused by field inhomogeneity (*15, 16*). Reconstruction software was implemented in C language on an SGI Indy computer. Image calculation includes the following steps:

(a) Time reversal of echoes acquired with negative readout gradient
(b) Sorting of echoes taken in all shots
(c) Zero filling to a 256 × 256 matrix
(d) Fast Fourier transform (FFT) in the readout direction (rows of the matrix)
(e) Nonlinear or linear phase correction of rows
(f) FFT in the phase encoding direction (columns)
(g) Magnitude calculation

Prior to the actual reconstruction, the nonlinear phase correction function $F(x)/|F(x)|$ is estimated according to Eq. [5], based on an image line selected by the operator. This requires two additional executions of the steps (d) and (f) to

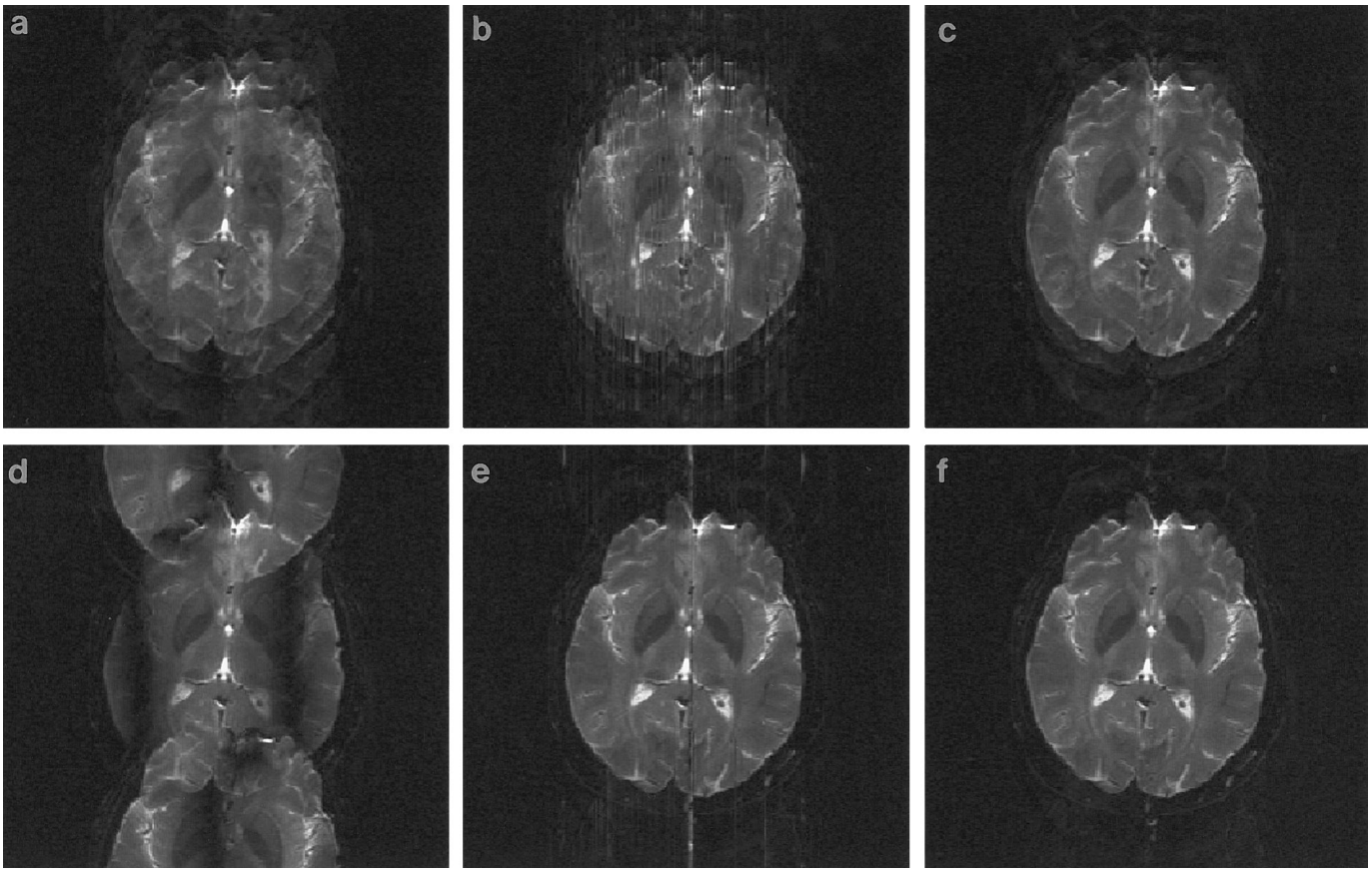

FIG. 5. Interleaved EPI of human head acquired with 9 shots using a misadjusted sequence. Upper row (a–c): standard interleaving scheme. Lower row (d–f): alternating interleaving. From left to right: raw reconstruction (a, d), reconstruction with a nonlinear phase correction derived from the bottom line (b, e), and reconstruction with linear phase correction derived by a fit to the nonlinear phase correction (c, f). The application of the alternating interleaving scheme reduces the number of ghosts to one, gives fewer errors in the calculation of the nonlinear phase correction, and allows a correct linear fit.

calculate images ρ_{even} and ρ_{odd}. However, when multiple repetitions of an image are processed (e.g., in a dynamic study), the estimation of the phase correction needs to be performed only once, so the net increase of the computation time caused by the redundant steps is negligible. Linear phase correction parameters are derived using a Fourier transform of $F(x)/|F(x)|$, and by taking the interpolated position of the highest peak (first-order term) and its phase (zero-order term), as described in Ref. *11*.

The experiments were purposely carried out without any timing adjustments of the sequence for even–odd echo shift compensation. The image obtained with the standard interleaving scheme and reconstructed without any phase correction (Fig. 5a) contains the typical effect of multiple ghosting. The edges of two primary ($m = -1, 0$) ghosts shifted up and down by 14 pixels (FOV/2n) are distinguishable, and the train of higher-order ghosts is visible as a smear of the image. An attempt was taken to calculate the nonlinear phase correction function based on the bottom line of the image. The image reconstructed with this correction contains numerous vertical streaks (Fig. 5b). These are a result of an erroneous estimation of the phase of $F(x)$ due to a low signal-to-noise ratio of ρ_{even} and ρ_{odd} profiles along the selected line. The linear phase fit to this noisy phase correction function failed to give the correct values of phase- and k-space shifts of even vs odd echoes. The linear-phase-corrected image (Fig. 5c) still suffers from a significant ghosting effect.

The image acquired with alternating trajectories and reconstructed without phase correction contains a single artifact shifted by FOV/2 as in the single shot EPI, as expected (Fig. 5d). The lack of multiple ghosts proves that the echoes acquired with the same gradient polarity are equivalent in alternate shots, as discussed in Theory. Again, the nonlinear phase correction was estimated based on the bottom line. This time, the estimation is much more precise. The image obtained with this nonlinear correction (Fig. 5e) contains just a few streaks, which appear in those positions where the selected line crosses some dark elements of the object (center) or does not contain information about its entire extent (edges). This is a typical problem of image-based phase correction, also occurring with single-shot data, and can easily be avoided by a linear (or higher order) phase fit. The application of the linear phase

correction, with parameters found by the Fourier fit described earlier, gave a practically ghost-free image (Fig. 5f). Parameters found by the fit were phase shift of 33° and a k_x shift of 3.0 samples. In the previously described experiment with the standard interleaving, the fit gave 72° and 2.8 samples, and thus an error of 39° and 0.2 samples.

The alternating interleaving scheme was proposed here to improve the sensitivity of the image-based phase correction in multishot EPI. However, it may also be advantageous even with the standard, reference scan based method for phase correction. If a residual artifact remains after the phase correction (e.g., due to a resonance offset or flow), it will be single and shifted by half the field of view, instead of being replicated n times along the phase encoding axis. The fact that a single ghost is less disturbing than a train of ghosts is immediately seen by a comparison of the uncorrected images (Figs. 5a and 5d). One should note, however, that the alternating interleaving scheme removes only the odd ghosts caused a mismatch of odd and even gradient echoes. Ghosts resulting from a lack of steady state or hardware instability will remain unaffected.

CONCLUSIONS

It is theoretically possible to correct an n-shot EPI data set for the phase inconsistency of even vs odd echoes using a phase correction derived from the ghosting artifact. However, two effects limit the applicability of this method in practice. First, its sensitivity to noise is at least n times higher than in a single-shot experiment because the calculation must be based on high order, low intensity ghosts which are sufficiently shifted from the original image. Second, the presence of "even ghosts" caused by signal variations can lead to errors in the estimation of the phase correction. The use of a modified interleaving scheme in which the initial direction of consecutive k-space trajectories is alternated and the number of interleaves is odd ensures that the phase inconsistency of even and odd echoes results in a single, strong ghost shifted by one-half of the field of view. With this modification, the image-based phase correction method can be applied to interleaved data with the same sensitivity to noise as in single-shot EPI experiments and the influence of even ghosts is reduced.

APPENDIX: EVEN-ECHO AND ODD-ECHO RECONSTRUCTIONS

Knowing that $\mathrm{III}(k)$ is invariant of FT, and that the FT of $\Pi(k)$ is $\mathrm{sinc}(y) = \sin(\pi y)/\pi y$, we find the Fourier transform of the distribution of even gradient echoes, $g_{\mathrm{even}}(k_y)$, given by Eq. [10] using convolution, shift, and similarity theorems:

$$G(y) = \mathrm{FT}[\,g_{\mathrm{even}}(k_y)] = \mathrm{III}(k_0 y) * [\,n k_0 e^{i2\pi y d}\,\mathrm{sinc}(n k_0 y)\,\mathrm{III}(2 n k_0 y)]. \quad [A1]$$

Note that

$$n k_0\,\mathrm{sinc}(n k_0 y)\,\mathrm{III}(2 n k_0 y) = \tfrac{1}{2}\,\delta(y) + \frac{1}{\pi}\sum_{l=-\infty}^{+\infty}\frac{(-1)^l}{2l+1}\,\delta\left[y - \frac{2l+1}{2 n k_0}\right] \quad [A2]$$

because the peaks of the III symbol coincide either with zeros or with lobe centers of the sinc. Writing the first III symbol in [A1] in the explicit form, we obtain

$$\begin{aligned} G(y) &= \sum_{p=-\infty}^{+\infty}\delta(y - p/k_0) * \left\{\tfrac{1}{2}\,\delta(y) + \frac{1}{\pi}\,e^{i2\pi y d} \times \sum_{l=-\infty}^{+\infty}\frac{(-1)^l}{2l+1}\,\delta\left[y - \frac{2l+1}{2 n k_0}\right]\right\} \\ &= \tfrac{1}{2}\sum_{p=-\infty}^{+\infty}\delta(y - p/k_0) + \frac{1}{\pi}\sum_{l=-\infty}^{+\infty}\sum_{p=-\infty}^{+\infty}\exp\left[\frac{i2\pi d(2l+1)}{2 n k_0}\right] \times \frac{(-1)^l}{2l+1}\,\delta\left[y - \frac{2(pn+l)+1}{2 n k_0}\right]. \end{aligned} \quad [A3]$$

We replace the summation over l by a summation over $m = pn + l$ and substitute FOV for $1/k_0$. Now,

$$G(y) = \tfrac{1}{2}\sum_{p=-\infty}^{+\infty}\delta(y - p\mathrm{FOV}) + \tfrac{1}{2}\sum_{m=-\infty}^{+\infty}A_m\,\delta\left[y - (2m+1)\,\frac{\mathrm{FOV}}{2n}\right], \quad [A4]$$

where

$$A_m = \frac{2}{\pi}\sum_{p=-\infty}^{+\infty}\exp\left\{i2\pi d[2(m - pn) + 1]\,\frac{\mathrm{FOV}}{2n}\right\} \times \frac{(-1)^{m-pn}}{2(m - pn) + 1}. \quad [A5]$$

As mentioned in the discussion following Eq. [11], two cases should be considered: n odd with $d = 0$, and n even with $d = 1/(2\ \mathrm{FOV})$. In the case of odd n,

$$A_m = \frac{2}{\pi}(-1)^m \sum_{p=-\infty}^{+\infty} \frac{(-1)^p}{2(m-pn)+1}$$
$$= \frac{(-1)^m}{n}\left[\frac{1}{\pi(2m+1)/(2n)} + \frac{2}{\pi}\sum_{p=1}^{\infty}\frac{(-1)^p(2m+1)/(2n)}{[(2m+1)/(2n)]^2 - p^2}\right]$$
$$= \frac{(-1)^m}{n\sin[\pi(2m+1)/(2n)]}, \qquad [A6]$$

where the last transition comes from Ref. (*17*). Similarly, for even n,

$$A_m = \frac{2}{\pi} e^{i\pi[(2m+1)/(2n)+m]} \sum_{p=-\infty}^{+\infty} \frac{(-1)^p}{2(m-pn)+1}$$
$$= \frac{e^{i\pi[(2m+1)/(2n)+m]}}{n\sin[\pi(2m+1)/(2n)]}. \qquad [A7]$$

The FT of the distribution of odd echoes can be easily derived from [11] and [A4] using the shift theorem:

$$FT[g_{\text{odd}}(k_y)] = e^{i2\pi yn/\text{FOV}} G(y)$$
$$= \tfrac{1}{2}\sum_{p=-\infty}^{+\infty}\delta(y - p\text{FOV}) - \tfrac{1}{2}\sum_{m=-\infty}^{+\infty} A_m \delta\left[y - (2m+1)\frac{\text{FOV}}{2n}\right]. \qquad [A8]$$

The images reconstructed separately from even and odd gradient echoes are given by the y-convolution of $\rho(x, y)$ with the transforms given by [A4] and [A8]. This means simply replacing δ's by ρ's in [A4] and [A8]. Additionally, if the object y-extents are smaller than FOV, only the replications within $\pm$FOV/2 are visible, so that only the terms with $p = 0$ and $m = -n/2 \ldots n/2 - 1$ (for n even), or $m = -(n-1)/2, \ldots (n-1)/2$ (for n odd) should be left. This gives Eqs. [12] and [13].

ACKNOWLEDGMENT

The author thanks Tomasz Skorka for helpful discussions.

REFERENCES

1. P. Mansfield, Multi-planar image formation using NMR spin echoes, *J. Phys. C: Solid State Phys.* **10,** L55–58 (1977).
2. P. Mansfield, Imaging by nuclear magnetic resonance, *J. Phys. E: Sci. Instrum* **21,** 18–21 (1988).
3. G. C. McKinnon, Ultrafast interleaved echo-planar imaging. *Magn. Reson. Med.* **30,** 609–616 (1993).
4. K. Butts, S. J. Riederer, R. L. Ehman, R. M. Thompson, and C. R. Jack, Interleaved EPI on a standard MRI system. *Magn. Reson. Med.* **31,** 67–72 (1994).
5. R. J. Ordidge, A. Howseman, R. Coxon, R. Turner, B. Chapman, P. Glover, M. Stehling, and P. Mansfield, Snapshot imaging at 0.5 T using echo-planar techniques. *Magn. Reson. Med.* **10,** 227–240 (1989).
6. H. Bruder, H. Fischer, H.-E. Reinfelder, and F. Schmitt, Image reconstruction for EPI with non-equidistant k-space sampling. *Magn. Reson. Med.* **23,** 311–323 (1992).
7. A. Jesmianowicz, E. C. Wong, and J. S. Hyde, Self-correcting EPI reconstruction algorithm, Proceedings, SMR and ESMRMB, Joint Meeting, Nice, p. 619, 1995.
8. O. Heid, Robust EPI phase correction, Proceedings of the International Society of Magnetic Resonance in Medicine, 5th Annual Meeting, Vancouver, p. 2014, 1997.
9. M. H. Buonocore and L. Gao, Ghost artifact reduction for echo planar imaging using image phase correction, *Magn. Reson. Med.* **38,** 89–100 (1997).
10. K. F. King, C. R. Crawford, and J. K. Maier, Correction of filter-induced ghosts in echo-planar imaging, Proceedings, SMR and ESMRMB Joint Meeting, Nice, p. 105, 1995.
11. F. Hennel, EPI deghosting by linear phase correction without reference scans, Proceedings of the International Society of Magnetic Resonance in Medicine, 5th Annual Meeting, Vancouver, p. 1808, 1997.
12. R. N. Bracewell, "The Fourier Transform and Its Applications," McGraw-Hill, Singapore (1986).
13. S. B. Reeder, E. Altar, B. D. Bolster, Jr., and E. R. McVeigh, Quantification and reduction of ghosting artifacts in interleaved echo-planar imaging, *Magn. Reson. Med.* **38,** 429–439 (1997).
14. B. Chapman and P. Mansfield, *J. Phys. D: Appl. Phys.* **19,** L129 (1986).
15. Z. H. Cho, C. B. Ahn, J. H. Kim, Y. E. Lee, and C. W. Mun, Phase error corrected interlaced EPI, Abstracts of the Society of Magnetic Resonance in Medicine, 6th Annual Meeting, New York, p. 912, 1987.
16. D. A. Feinberg and K. Oshio, Phase-errors in multi-shot EPI, *Magn. Reson. Med.* **32,** 535–539 (1994).
17. I. S. Gradshteyn, I. M. Ryzhik, "Tables of Integrals, Series, and Products," Academic Press, New York (1980).